Activation of nuclear factor-κB during doxorubicin-induced apoptosis in endothelial cells and myocytes is pro-apoptotic: the role of hydrogen peroxide

Suwei WANG, Srigiridhar KOTAMRAJU, Eugene KONOREV, Shasi KALIVENDI, Joy JOSEPH and Balaraman KALYANARAMAN[1]

Biophysics Research Institute and Free Radical Research Center, Medical College of Wisconsin, 8701 Watertown Plank Road, Milwaukee, WI 53226, U.S.A.

Doxorubicin (DOX) is a widely used anti-tumour drug. Cardiotoxicity is a major toxic side effect of DOX therapy. Although recent studies implicated an apoptotic pathway in DOX-induced cardiotoxicity, the mechanism of DOX-induced apoptosis remains unclear. In the present study, we investigated the role of reactive oxygen species and the nuclear transcription factor nuclear factor κB (NF-κB) during apoptosis induced by DOX in bovine aortic endothelial cells (BAECs) and adult rat cardiomyocytes. DOX-induced NF-κB activation is both dose- and time-dependent, as demonstrated using electrophoretic mobility-shift assay and luciferase and p65 (Rel A) nuclear-translocation assays. Addition of a cell-permeant iron metalloporphyrin significantly suppressed NF-κB activation and apoptosis induced by DOX. Overexpression of glutathione peroxidase, which detoxifies cellular H_2O_2, significantly decreased DOX-induced NF-κB activation and apoptosis. Inhibition of DOX-induced NF-κB activation by a cell-permeant peptide SN50 that blocks translocation of the NF-κB complex into the nucleus greatly diminished DOX-induced apoptosis. Apoptosis was inhibited when IκB mutant vector, another NF-κB inhibitor, was added to DOX-treated BAECs. These results suggest that NF-κB activation in DOX-treated endothelial cells and myocytes is pro-apoptotic, in contrast with DOX-treated cancer cells, where NF-κB activation is anti-apoptotic. Removal of intracellular H_2O_2 protects endothelial cells and myocytes from DOX-induced apoptosis, possibly by inhibiting NF-κB activation. These findings suggest a novel mechanism for enhancing the therapeutic efficacy of DOX.

Key words: Fe(III)tetrakis(4-benzoic acid)porphyrin (FeTBAP), glutathione peroxidase-1 (GPx-1), NF-κB, superoxide dismutase-mimetic.

INTRODUCTION

Doxorubicin (DOX), a broad-spectrum anti-tumour antibiotic, has been widely used to treat various cancers [1]. A major adverse side effect of DOX treatment in cancer patients is the onset of cardiomyopathy and heart failure [2]. Reactive oxygen species (ROS) derived from redox activation of DOX were proposed to be responsible for DOX cardiotoxicity [3–6]. Previous studies have indicated that, at submicromolar concentrations, DOX induces caspase-dependent apoptotic signalling in endothelial cells and myocytes [7,8]. Efforts to understand the signal-transduction pathways responsible for DOX-induced apoptosis are underway in several laboratories [9–11].

One of the major signal-transduction pathways that is activated in response to oxidant stress is that of the nuclear transcription factor nuclear factor κB (NF-κB), which is crucial for cell survival, cell proliferation and immune responses via expression of its target genes [12,13]. In quiescent cells, the active form of NF-κB in cytosol remains bound to the inhibitory molecule, IκBα (inhibitor of NF-κB) [13]. Upon stimulation by pro-inflammatory cytokines or oxidants, IκBα is phosphorylated by the upstream kinase, IκB kinase (IKK), which leads to the polyubiquitination and degradation of IκB by proteases, causing the release and translocation of NF-κB complex into the nucleus [13]. Activated NF-κB subsequently binds to specific DNA sequences and regulates the expression of its target genes, which mediate inflammatory response, apoptosis and carcinogenesis.

The activation of NF-κB either promotes or blocks apoptotic cell death, depending upon the cell type and the nature of oxidative stimuli [14,15]. Recent studies have shown that inhibition of NF-κB activation sensitized DOX-induced apoptosis in various cancer cells (e.g. breast cancer, pancreatic cancer, renal and hepatocellular carcinoma) [16–18]. These results implicate an anti-apoptotic role for NF-κB in DOX-induced apoptosis in tumour cells. In the literature, there exists a precedent for the anti-apoptotic role of NF-κB, which is presumably mediated by target genes responsible for regulation of cell proliferation and cell survival [13,19]. However, conflicting results have also been reported on the role of NF-κB in endothelial apoptosis [19–21].

In the present study, we investigated the effect of NF-κB in DOX-induced apoptosis in endothelial cells and cardiomyocytes. Our results provide evidence for the first time that NF-κB activation is pro-apoptotic in DOX-treated endothelial cells and cardiomyocytes, and strongly suggest that H_2O_2 is responsible for DOX-induced NF-κB activation. Therapeutic implications of selective modulation of NF-κB levels and apoptosis in tumour cells and cardiovascular cells are discussed.

EXPERIMENTAL

Materials

DOX was purchased from Sigma (St. Louis, MO, U.S.A.). SN50 and SN50M were purchased from Biomol Research Laboratories

Abbreviations used: BAEC, bovine aortic endothelial cell; DMEM, Dulbecco's modified Eagle's medium; DOX, doxorubicin; DTT, dithiothreitol; FBS, fetal bovine serum; FeTBAP, Fe(III)tetrakis(4-benzoic acid)porphyrin; GPx-1, glutathione peroxidase-1; IκB, inhibitor of NF-κB; IKK, IκB kinase; L-NAME, N^G-nitro-L-arginine methyl ester; NF-κB, nuclear factor κB; PDTC, pyrrolidine dithiocarbamate; ROS, reactive oxygen species; TNF-α, tumour necrosis factor-α; TUNEL, terminal deoxynucleotidyltransferase-mediated nick-end labelling.

[1] To whom correspondence and reprint requests should be addressed (e-mail balarama@mcw.edu).

(Plymouth Meeting, PA, U.S.A.). Fe(III)tetrakis(4-benzoic acid)porphyrin (FeTBAP) was synthesized according to the method published previously [22]. All antibodies were purchased from Santa Cruz Biotechnology (Santa Cruz, CA, U.S.A.). Glutathione peroxidase-1 (GPx-1) expression plasmid was generously given by Dr Larry Oberley (University of Iowa, IA, U.S.A.). IκB mutant (S32 and S36) and IκB empty vectors were obtained from Dr Galen M. Pieper (Medical College of Wisconsin, WI, U.S.A.).

Endothelial cell culture

Bovine aortic endothelial cells (BAECs) were obtained from Clonetics, San Diego, CA, U.S.A. Cells were cultured in Dulbecco's modified Eagle's medium (DMEM) containing 15% (v/v) fetal bovine serum (FBS), L-glutamine (2 mM), penicillin (100 units/ml) and streptomycin (100 μg/ml), and incubated at 37 °C in a humidified atmosphere of CO_2/air (1:19). All experiments were performed in a similar medium containing 2% FBS.

Myocyte isolation and culture

Male Harlan Sprague–Dawley adult rats were anaesthetized with pentobarbital (60 mg/kg intraperitoneal), and hearts were excised and placed into ice-cold saline solution [23]. Hearts were mounted on aortic cannulas and perfused with perfusion buffer [125 mM NaCl/25 mM Hepes (pH 7.4)/11 mM glucose/5 mM creatine/20 mM taurine/4.7 mM KCl/1.2 mM $MgSO_4$/1.2 mM KH_2PO_4], which was saturated with 100% oxygen. After a 10 min perfusion, the perfusion buffer was changed to a Ca^{2+}-free buffer. After a 5 min perfusion with Ca^{2+}-free buffer, the perfusion was continued by recirculation of 40 ml of buffer supplemented with collagenase (type II; Life Technologies, Grand Island, NY, U.S.A.) and 25 μM $CaCl_2$, as described previously [23]. After 30 min, ventricular tissue was minced and incubated for 10 min in a recirculating medium with 1% (w/v) BSA and 20 μg/ml deoxyribonuclease (Sigma). Cells were released from chunks of tissue by gentle pipetting. The cell suspension was filtered through an 80-mesh screen. The cell suspension was washed twice by gentle centrifugation and resuspended in a $CaCl_2$-containing buffer. The concentration of $CaCl_2$ in the buffer was successively increased to 0.2 and 0.5 mM. To separate myocytes, the cell suspension was layered over a 4% (w/v) BSA solution in a perfusion buffer containing 1 mM $CaCl_2$. Ventricular myocytes were allowed to settle and then plated on to four-well chamber slides or 100 mm dishes precoated with laminin (Life Technologies). The culture medium contained M-199 (Sigma) supplemented with 25 mM $NaHCO_3$, 25 mM Hepes, 10% FBS, 2 mM L-carnitine, 5 mM creatine, 5 mM taurine, 2 mM glutamine, 0.1 μM insulin, 10 μM cytosine-β-D-arabinofuranoside, 100 units/ml penicillin and 100 μg/ml streptomycin. Intact cardiomyocytes adhered to the culture plates; damaged cells were washed away during the medium change 2 h after plating. Cardiomyocytes were cultured under these conditions for 7–10 days and starved in 2% FBS culture medium overnight before treatments.

Nuclear extraction

Nuclear extracts were prepared by a modified method, as reported recently [24]. The cells were cultured in 100 mm cell culture plates at 5×10^6 cells/plate for 24 h. After treatment, cells were harvested by scraping in 1 ml of buffer A [10 mM Hepes/1.5 mM $MgCl_2$/10 mM KCl/0.5 mM PMSF/10 ng/ml leupeptin/10 ng/ml aprotinin/0.5 mM dithiothreitol (DTT)]. After centrifugation at 14000 ***g*** for 2 min at 4 °C, the cell pellet was resuspended in 60 μl of buffer A with 0.1% (v/v) Nonidet P40 and incubated on ice for 10 min. After centrifugation at 14000 ***g*** for 10 min, the supernatant was saved in 90 μl of buffer D [20 mM Hepes/0.05 mM KCl/20% (v/v) glycerol/0.2 mM EDTA/0.5 mM PMSF/10 ng/ml leupeptin/10 ng/ml aprotinin/0.5 mM DTT] as a cytoplasmic extract. The nuclear pellet was then resuspended in 60 μl of buffer C [20 mM Hepes/1.5 mM $MgCl_2$/0.42 M NaCl/0.2 mM EDTA/25% (v/v) glycerol/0.5 mM PMSF/10 ng/ml leupeptin/10 ng/ml aprotinin/0.5 mM DTT], and incubated on ice for 10 min. After centrifugation at 14000 ***g*** for 10 min, the supernatant was collected in 90 μl of buffer D, and this nuclear protein extract was stored at −70 °C. The concentration was determined using a bicinchoninic acid (BCA) protein assay reagent (Pierce, Rockford, IL, U.S.A.).

Electrophoretic mobility-shift assay

The double-stranded NF-κB oligonucleotide with binding sequence of 5′-AGTTGAGGGGACTTTCCCAGGC-3′ was purchased from Promega (Madison, WI, U.S.A.). The oligonucleotide was labelled with [^{32}P]P_i using Redivue [γ-^{32}P]ATP (Amersham Biosciences, Piscataway, NJ, U.S.A.) and DNA 5′-end labelling system (Promega).

The DNA–protein-binding reaction was conducted in a 20 μl reaction mixture including 3 μg of poly(dI/dC) (Sigma), 10 μg of nuclear protein extract, 4×10^4 c.p.m. of ^{32}P-labelled oligonucleotide probe (1 μl) and 2 μl of 10 × gel-shift running buffer [100 mM Tris/HCl (pH 7.5)/400 mM NaCl/10 mM EDTA/10 mM DTT]. This mixture was incubated for 30 min at room temperature, and then 2 μl of dye [25 mM Tris/HCl (pH 7.5)/50% (v/v) glycerol/0.1% Bromophenol Blue] was added to stop the reaction. The DNA–protein complexes were resolved on a 4% polyacrylamide gel, and the loaded gel was run at 140 V for 2 h in 0.5 × Tris/boric acid/EDTA buffer. The gel was then dried and placed on Kodak X-OMAT film (Eastman Kodak, Rochester, NY, U.S.A.) for autoradiography. The film was developed after overnight exposure at −70 °C.

Luciferase assay

BAECs (1×10^5) suspended in 1 ml of DMEM medium containing 15% (v/v) FBS were seeded into each well of a 12-well plate. After incubating at 37 °C for 24 h, the cells were transiently transfected with 1 μg of NF-κB–luciferase reporter plasmid and 1 μg of β-gal plasmid in DMEM medium without FBS, and antibiotics using the LIPOFECTAMINE™ reagent (Life Technologies). The cells were incubated for 4 h, and then fresh DMEM/15% FBS medium was added. After 24 h, the cells were starved for a further 24 h in 2% (v/v) FBS/DMEM medium, followed by exposure to different treatments. The luciferase activity was determined using the luciferase assay system with reporter lysis buffer from Promega. Briefly, the cells were harvested by scraping in 200 μl of reporter lysis buffer into a 1.5 ml microcentrifuge tube, vortex-mixed for 15 s, centrifuged at 12000 ***g*** for 30 s, and then the supernatant cell lysates were collected. The luciferase activity was measured with 60 μl of cell lysate and 20 μl of substrate using a Monolight luminometer. β-Galactosidase activity was determined as described previously [25]. The results are expressed as relative NF-κB activity com-

pared with controls after normalizing for β-galactosidase activity and protein concentration.

Kinase assay

DOX-treated BAECs were transferred on to ice, washed once with cold PBS and lysed in lysis buffer [50 mM Hepes/2 mM $MgCl_2$/1 mM EDTA/150 mM NaCl/10 mM Na_3VO_4/1 mM PMSF/0.1 % Nonidet P40/10 μg/ml leupeptin/10 μg/ml aprotinin/0.5 mM DTT/100 μM NaF]. After centrifugation at 14000 ***g*** at 4 °C for 10 min, the supernatants were collected and protein concentrations were determined, as reported previously. IKK was immunoprecipitated from 200 μg of protein with an IKKγ antibody at 4 °C for 2 h using Protein A–agarose beads (Amersham Biosciences). The precipitates were washed once with a lysis buffer and a kinase buffer (20 mM Hepes/20 mM 2-glycerophosphate/1 mM $MnCl_2$/5 mM $MgCl_2$/1 mM DTT/2 mM NaF). The kinase reaction was performed using 1 μg of glutathione S-transferase–IκBα (obtained as a gift from Dr Yvonne Janssen-Heininger, University of Vermont, VT, U.S.A.) and 5 μCi of [γ -^{32}P]ATP at 30 °C for 30 min. Reactions were terminated by the addition of 2 × Laemmli's sample buffer [2 % (w/v) SDS/10 % (v/v) glycerol/50 μM DTT/0.01 % Bromophenol Blue]. Samples were then boiled and stored at −20 °C. Proteins were separated on a 15 % (w/v) polyacrylamide gel, and gels were dried and exposed to the film for autoradiography. The film was developed after overnight exposure at −70 °C.

Detection of p65 nuclear translocation

The cells were seeded into each well of the four-well plastic chamber slides (Fisher Scientific, Pittsburgh, PA, U.S.A.), and incubated at 37 °C for 24 h. After starving in 2 % FBS/DMEM for 24 h, the cells were exposed to different treatments. After washing, the cells were fixed in 1 % (v/v) formalin in PBS for 10 min. The fixed cells were incubated with a 10 % blocking buffer (non-fat milk in PBS) for 20 min to suppress non-specific binding. The cells were then incubated with 2 μg/ml p65 antibody in a 1.5 % blocking buffer for 1 h, followed by incubation with 5 μg/ml fluorescein-conjugated secondary antibody in a 1.5 % blocking buffer for 45 min. The p65 protein exhibits strong green fluorescence, which can be detected by fluorescence microscopy. Both phase contrast and fluorescence microscopy were utilized to investigate the whole cell at the same time.

Terminal deoxynucleotidyltransferase-mediated nick-end labelling (TUNEL) assay

The TUNEL assay was used for microscopic detection of apoptosis [26]. This assay is on the basis of labelling of 3′-free hydroxyl ends of the fragmented DNA with fluorescein-dUTP catalysed by terminal deoxynucleotidyltransferase. Procedures were followed as described by the manufacturers of the ApoAlert DNA fragmentation assay kit (ClonTech Laboratories, Palo Alto, CA, U.S.A.). Apoptotic cells exhibit a strong nuclear green fluorescence that can be detected using a standard fluorescein filter (520 nm). All cells stained with propidium iodide exhibit a strong red cytoplasmic fluorescence at 620 nm. The areas of apoptotic cells were detected by fluorescence microscopy equipped with rhodamine and FITC filters. The photographs and quantification of apoptosis were obtained using a MetaMorph Imaging System (Universal Imaging Corp., West Chester, PA, U.S.A.).

Caspase-3 activity

The caspase-3-like activity is increased via a protease cascade during apoptosis in its early stage [27]. Following treatment with DOX and other antioxidants, cells were washed with ice-cold PBS and lysed with cell-lysis buffer (caspase-3 assay kit; Sigma). Samples were incubated on ice for 10 min and centrifuged in a microcentrifuge at 12000 ***g*** for 3 min at 4 °C to precipitate out the cellular debris. The caspase-3 activity in the supernatant was measured in a spectrophotometer, using Asp-Glu-Val-Asp-*p*-nitroanilide as a substrate, according to the manufacturer's instructions provided with the assay kit.

RESULTS

DOX-induced dose- and time-dependent NF-κB activation in BAECs and cardiomyocytes

The activation of NF-κB was measured in terms of its DNA-binding activity and the ability to promote the target gene expression. BAECs were incubated with 0.5 μM DOX for different time periods, and the DNA-binding activity was monitored in the nuclear extracts. As shown in Figure 1, the DNA-binding activity of NF-κB increased with time in DOX-treated endothelial cells (panels A and B) and cardiomyocytes (panels D and E). Supershift assay with p65 antibody suggests that the upper band is a p65/p50 heterodimer, which has a major role in NF-κB activity (Figure 1A). Figure 1(C) shows the results of the luciferase assay for NF-κB activity, which measures the ability of NF-κB as a transcription factor to regulate the expression of its target genes. Cells transiently transfected with NF-κB luciferase plasmid were exposed to different concentrations of DOX for 24 h. As shown in Figure 1(C), DOX induced a dose-dependent activation of NF-κB.

Next, we investigated the immunostaining of p65 protein, which provides a visual detection of the location of NF-κB in BAECs and myocytes. In quiescent cells, NF-κB resides in the cytoplasm as a heterodimer, mostly composed of p50 and p65 subunits. Upon activation, the active transcription factor translocates and binds to a specific DNA sequence in the nucleus and promotes target gene expression. In unstimulated cells, the NF-κB resides predominantly in the cytoplasm (Figures 2A and 2B, panels labelled 'Control'). After a 4 h treatment with 0.5 μM DOX, the translocation of NF-κB from cytoplasm to nuclei was apparent, which was monitored by tracking a strong green fluorescence in the nuclei (Figures 2A and 2B).

These findings indicate that DOX causes both the time- and dose-dependent activation of NF-κB (i.e. DNA-binding activity, transactivation ability and nuclear translocation) in endothelial cells and cardiomyocytes.

Antioxidants inhibit DOX-induced NF-κB activation

To investigate the role of ROS in DOX-induced NF-κB activation, we used a redox-active metalloporphyrin, FeTBAP, which was reported to detoxify superoxide, H_2O_2 and peroxynitrite [28,29]. Pre-incubation of endothelial cells or myocytes with 10 μM FeTBAP significantly decreased the DOX-induced NF-κB DNA-binding activity by 47 % and transactivation ability by 57 % (Figures 3A–3C). In addition, the translocation of NF-κB into the nuclei was inhibited in the presence of FeTBAP (Figure 3D).

Alternatively, we varied the levels of GPx-1, an intracellular enzymic scavenger of H_2O_2, by introducing the GPx-1 expression plasmid into BAECs [30]. In GPx-1-transfected cells treated with DOX, a dramatic decrease in the NF-κB DNA-

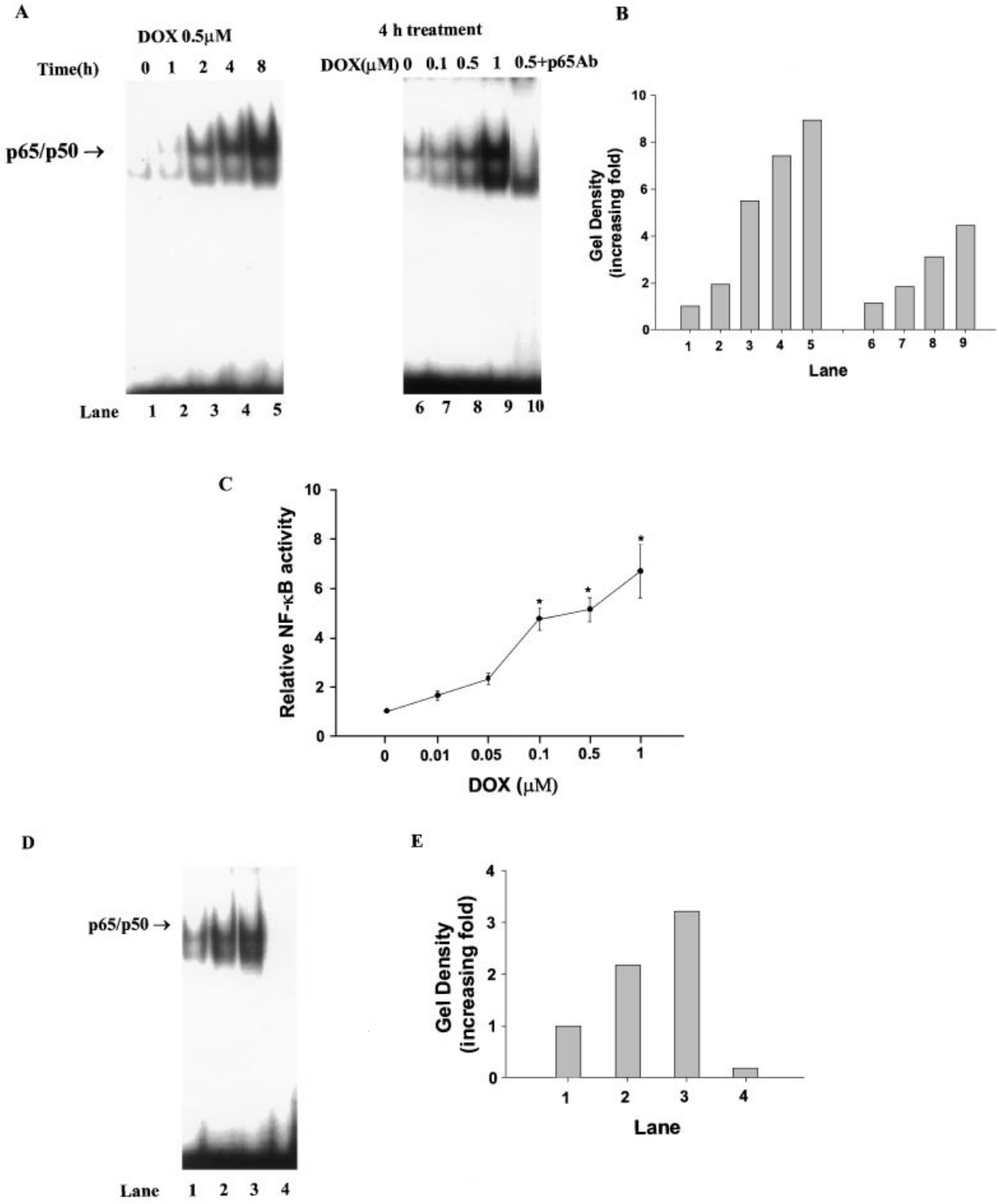

Figure 1 DOX-induced NF-κB activation in BAECs and cardiomyocytes

(**A**) BAECs were adjusted to a density of 1×10^6/ml and treated with different concentrations of DOX (0.1–1 μM) and with DOX (0.5 μM) for different time periods. After the incubation period, the nuclear extraction proteins were collected and used for DNA-binding activity assays. Supershift assay by p65 antibody (p65Ab; 100 μg/ml) assigned the upper band to p65/p50 heterodimer, which is responsible for the majority of NFκB activity. (**B**) Gel density quantification of different lanes shown in (**A**). (**C**) The luciferase assay for DOX-induced NF-κB activation. BAECs were transiently transfected with NF-κB luciferase reporter plasmid and β-gal plasmid. The cells were exposed to various concentrations of DOX for 16 h, and the NF-κB activity was measured by the luciferase activity assay. Results are presented as relative NF-κB induction compared with the untreated control cells (means $\pm$ S.E.M. for three repeated assays). Asterisks indicate a significant increase from the control ($P < 0.05$). (**D**) DOX-induced NF-κB activation in cardiomyocytes. The cardiomyocytes were treated with different concentrations of DOX for 4 h. The nuclear extraction proteins were collected and used for DNA-binding activity assays. Lane 1, control; lane 2, DOX (0.5 μM); lane 3, DOX (1 μM); and lane 4, cold probe. (**E**) Gel density quantification of different lanes shown in (**D**). All gel density quantifications were made using the upper p65/p50 bands.

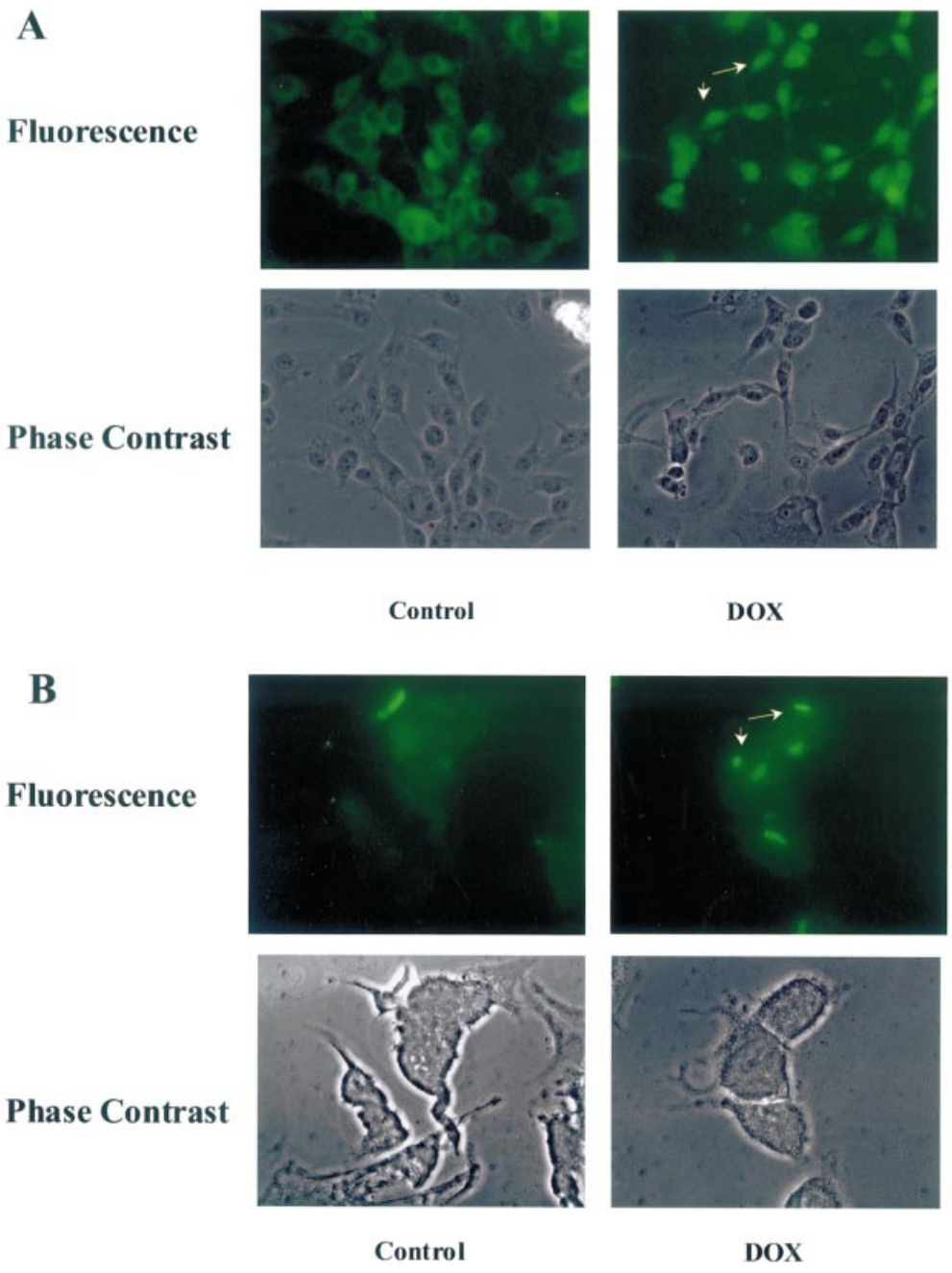

Figure 2 DOX-induced p65 nuclear translocation

(**A**) BAECs were exposed to 0.5 μM DOX for 4 h. The cells were subsequently incubated with p65 antibody and fluorescein-conjugated secondary antibody. The images were obtained either by fluorescence or by phase-contrast microscopy. The green fluorescence indicates the location of p65 protein. White arrows indicate the nuclear p65. (**B**) The same as in (**A**), except that cardiomyocytes were used in these experiments.

binding activity was observed (Figure 3A). These results indicate that both chemical and enzymic detoxification of H_2O_2 inhibit DOX-induced NF-κB activation.

DOX-induced NF-κB activation remained unaffected in BAECs and myocytes treated with N^G-nitro-L-arginine methyl ester (L-NAME), a non-specific inhibitor of all isoforms of nitric oxide synthase (results not shown). This observation is consistent with our earlier report showing a lack of effect of L-NAME in DOX-induced apoptosis and oxidative stress [7,31]. These results suggest that neither nitric oxide nor nitric oxide-derived oxidants (e.g. peroxynitrite) are responsible for DOX-induced NF-κB activation in BAECs and myocytes.

DOX-induced apoptosis and caspase-3 activation are inhibited by the antioxidants FeTBAP and GPx-1

In agreement with a previous report [7], we observed that DOX could induce apoptosis at very low concentrations (0.1–1 μM).

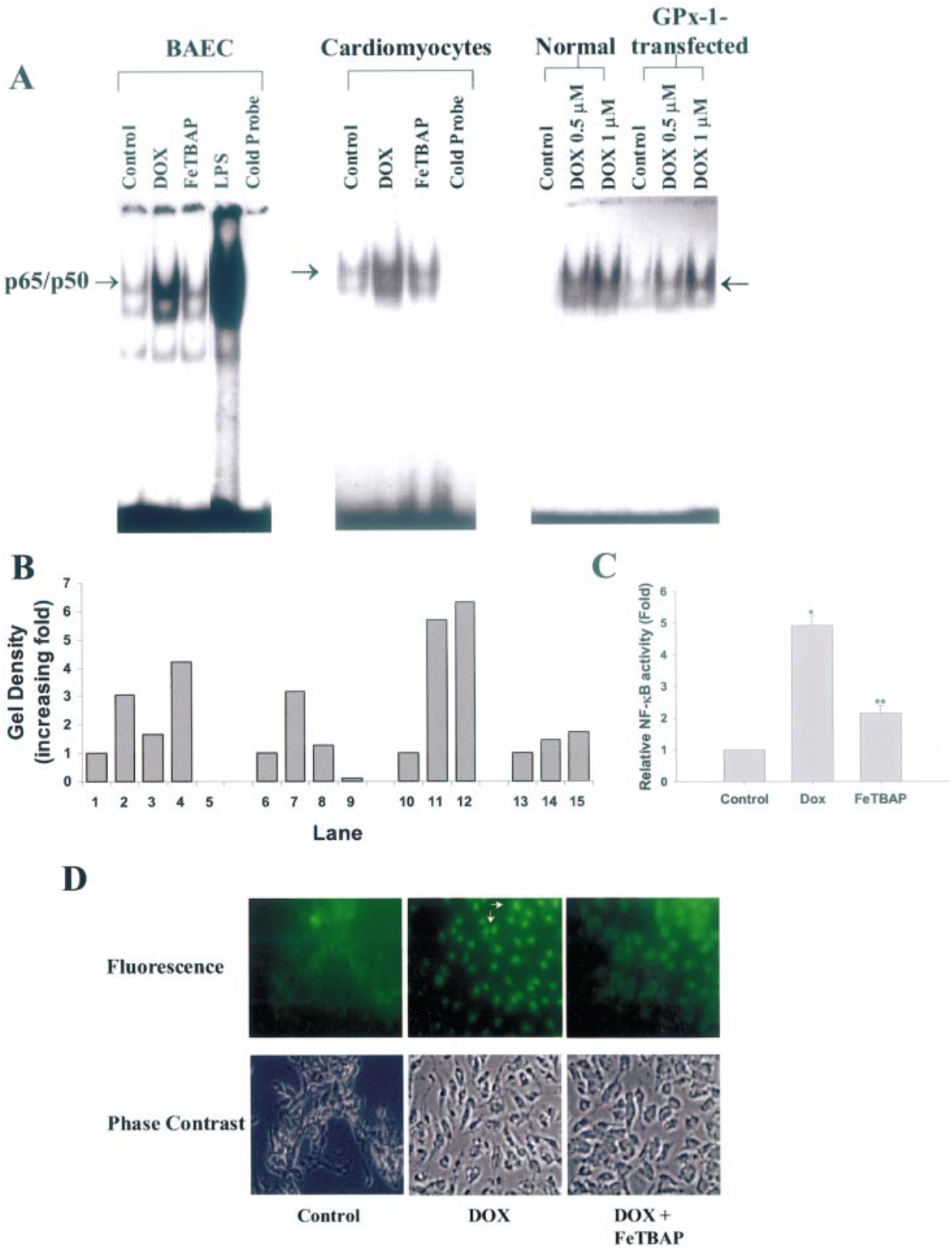

Figure 3 FeTBAP and GPx-1 block DOX-induced NF-κB activation

(**A**) BAECs and myocytes were pre-treated with 10 μM FeTBAP for 2 h. The cells were subsequently exposed to 0.5 μM DOX for 4 h, the nuclear extraction proteins were collected, and then used for the DNA-binding activity assay. BAECs were transfected with the GPx-1 expression plasmid. Following the transfection, the cells were treated with different concentrations of DOX for 4 h, and the nuclear extracts were collected for DNA-binding activity assay. (**B**) Gel density quantification of (**A**). (**C**) The luciferase assay for DOX-induced NF-κB activation. Transfected BAECs were pre-treated for 2 h with FeTBAP, followed by exposure to 0.5 μM DOX for 16 h, and the NF-κB activity was measured by luciferase activity assay. The single asterisk indicates a significant increase from control; the double asterisk indicates a significant decrease from DOX treatment. (**D**) FeTBAP blocks DOX-induced p65 nuclear translocation. After 2 h pre-treatment with FeTBAP, the cells were exposed to 0.5 μM DOX for 4 h and incubated with p65 antibody and fluorescein-conjugated secondary antibody. The images were obtained either by fluorescence or by phase-contrast microscopy. The green fluorescence indicates the location of p65 protein. White arrows indicate the nuclear p65.

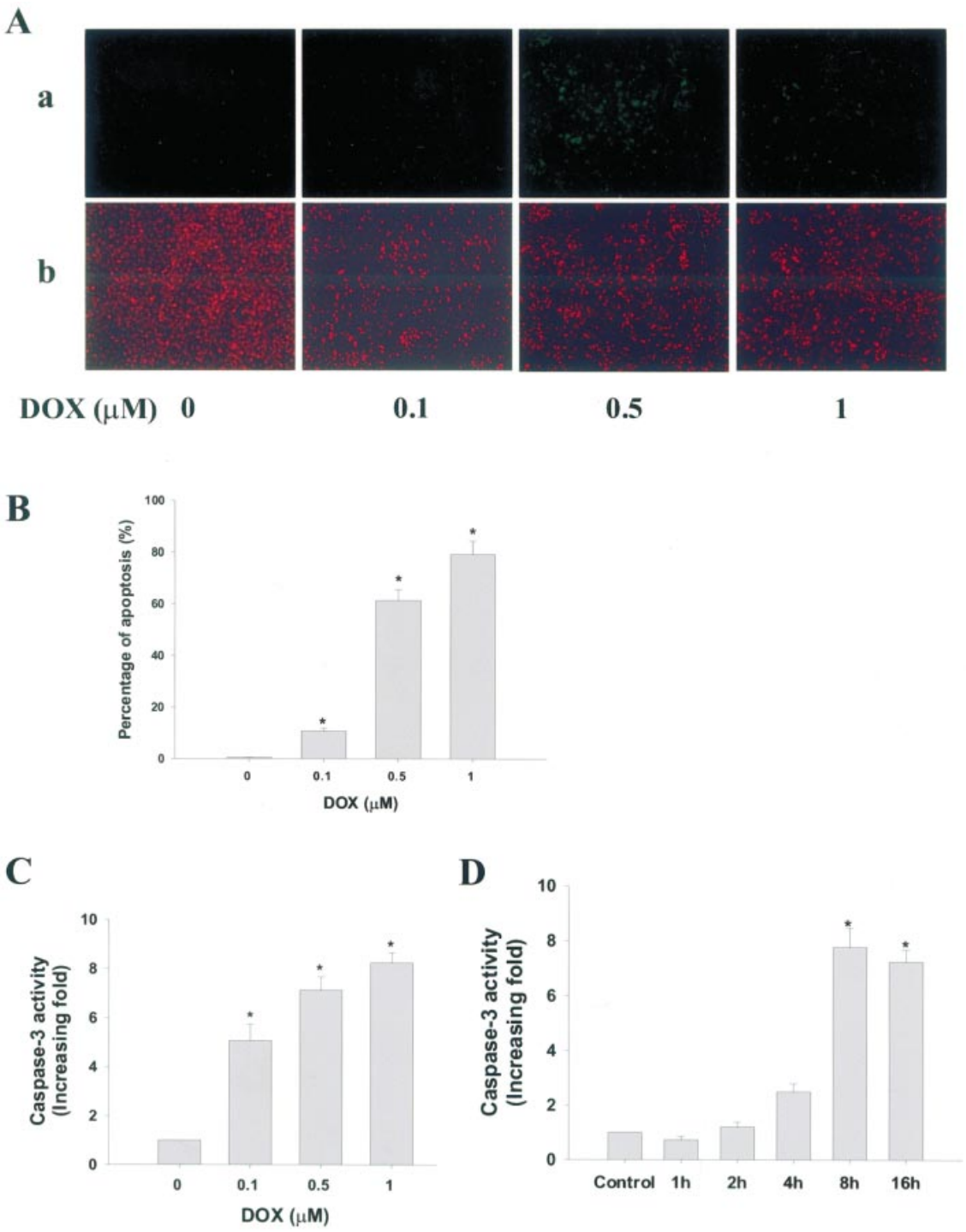

Figure 4 DOX-induced apoptosis and caspase-3 activation in BAECs

(**A**) BAECs were treated for 16 h with different concentrations of DOX as indicated, harvested, stained for TUNEL-positive cells and examined by fluorescence microscopy (**a**) or with propidium iodide staining (**b**). (**B**) The percentage quantification of apoptotic nuclei shown in (**A**). (**C**) and (**D**) DOX-induced caspase-3 activity in BAECs as a function of concentration and time respectively. BAECs were treated for 16 h with different concentrations of DOX, or with 0.5 μM DOX for different incubation times, as indicated, harvested, and caspase-3 activity was measured.

Apoptosis was measured using the TUNEL technique. As shown in Figure 4(A), following a 16 h incubation with 0.1 μM DOX, a significant increase in TUNEL-positive (apoptotic) cells from 0.5 to 10.8 % was detected. Exposure to different concentrations of DOX (0.5 and 1 μM) increased the percentage of apoptotic cells to 61.4 % and 79.2 % respectively (Figure 4B).

Next, we investigated the effect of DOX on caspase-3 activation, since caspase-3 is an important upstream factor leading

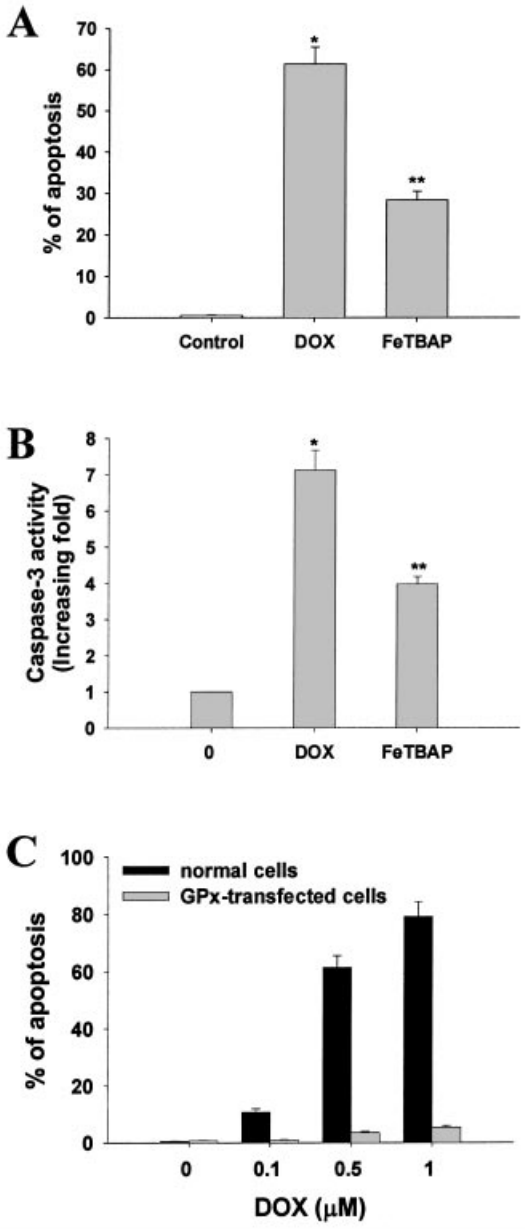

Figure 5 FeTBAP and GPx-1 overexpression inhibit DOX-induced apoptosis

(**A**) BAECs were treated with 10 μM FeTBAP for 2 h and with DOX (1 μM) for 16 h, harvested, stained for TUNEL-positive cells, and examined by fluorescence microscopy. Similar treatments were performed with DOX in the absence of FeTBAP. The average intensity values were obtained from three different fields of view obtained using Metamorph software. (**B**) The caspase-3 activity was measured under conditions described in (**A**). (**C**) BAECs were transfected with the GPx-1 plasmid. Following the transfection, cells were treated with different concentrations of DOX, as indicated, for 16 h and apoptosis was measured using the TUNEL assay. DOX-dependent apoptosis was quantified in control BAECs and GPx-1-transfected BAECs.

to apoptosis [32,33]. Consistent with the TUNEL assay, we found that 0.1 μM DOX caused a significant increase in caspase-3 activation after a 16 h incubation. The activation of caspase-3 increased with increasing concentration of DOX and increasing time of incubation (Figures 4C and 4D).

The fraction of TUNEL-positive cells and caspase-3 activation induced by DOX was decreased in the presence of FeTBAP (Figures 5A and 5B). Overexpression of GPx-1 almost completely inhibited the apoptosis induced by DOX (Figure 5C), suggesting that intracellular H_2O_2 was responsible for DOX-induced apoptosis in these cells.

Inhibition of DOX-induced apoptosis and caspase-3 activation by NF-κB inhibitor

To investigate the role of NF-κB in DOX-induced cellular response, we used a cell-permeant inhibitory peptide, SN50, and a cell-permeable control peptide, SN50M. BAECs were pre-incubated with either 25 μg/ml SN50 or SN50M for 30 min, and then treated with 0.5 μM DOX for 4 h. Pre-incubation with SN50 completely reversed the DNA-binding activity induced by DOX, whereas SN50M had a minimal inhibitory effect that was considerably less than that of SN50 (Figure 6A). Pre-incubation with SN50 significantly lowered the percentage of apoptosis from 61.4 to 18.1 % and 79.2 to 19.3 % in cells exposed to 0.5 μM and 1 μM DOX (Figure 6D). On the other hand, the control peptide SN50M exhibited a minimal inhibitory effect on DOX-induced apoptosis (Figure 6D). Despite causing a slight increase in the basal caspase-3 activity, the NF-κB inhibitory peptide SN50 dramatically blocked DOX-induced caspase-3 activation (Figure 6C). In addition to using the peptide inhibitor SN50, we used IκB mutant (S32 and S36) vector and IκB empty vector expression to investigate the pro-apoptotic role of NF-κB. As shown in Figures 6(B) and 6(E), the IκB mutant strongly inhibited DOX-induced NF-κB activation and significantly reduced DOX-induced apoptosis. In contrast, the negative control (i.e. IκB empty vector expression) had a minimal effect (Figures 6B and 6E). These results confirm that NF-κB activation functions as a pro-apoptotic factor in DOX-induced apoptosis.

DISCUSSION

In the present study, we demonstrate that DOX induces NF-κB activation in endothelial cells and cardiomyocytes. The NF-κB activation is mediated by DOX-induced H_2O_2. Antioxidants that caused a decrease in H_2O_2 formation in this system suppressed NF-κB activation and apoptosis. These findings strongly implicate NF-κB activation as a pro-apoptotic factor in DOX-treated endothelial cells and myocytes, as described in Scheme 1.

Numerous reports indirectly support the notion that intracellular ROS lead to the activation of NF-κB [34–37]. The link between ROS and NF-κB was established mainly from the inhibition of NF-κB activation by antioxidants and by overexpression of antioxidant enzymes {e.g. GPx-1 and manganese-containing superoxide dismutase ('MnSOD'); [38]}. The activation of NF-κB by tumour necrosis factor-α (TNF-α) in JB6 cells was inhibited by overexpression of catalase, a specific H_2O_2 scavenger [34]. Superoxide anion was reported to be responsible for TNF-α-induced NF-κB activation in macrophages [35]. Reports also indicate that hydroxyl radical acted as the secondary messenger for NF-κB activation in three different cells, including Jurkat cells, macrophages and JB6 cells, in response to various stimuli, such as exposure to Cr(VI), silica and ZnO [36].

Results from the present study indicate that, in DOX-treated endothelial cells and cardiomyocytes, intracellular H_2O_2 has a critical role in mediating DOX-induced NF-κB activation. Pre-incubation with FeTBAP, a cell-permeant metalloporphyrin antioxidant enzyme-mimetic, dramatically decreased DOX-induced NF-κB activation. FeTBAP, a redox-active metalloporphyrin, consists of a redox-active iron (III) located at the centre of a porphyrin ring. Recent reports indicate that FeTBAP is an efficient scavenger of both superoxide and H_2O_2 [28,31]. We have shown, using the ESR/'spin-trapping' technique, that

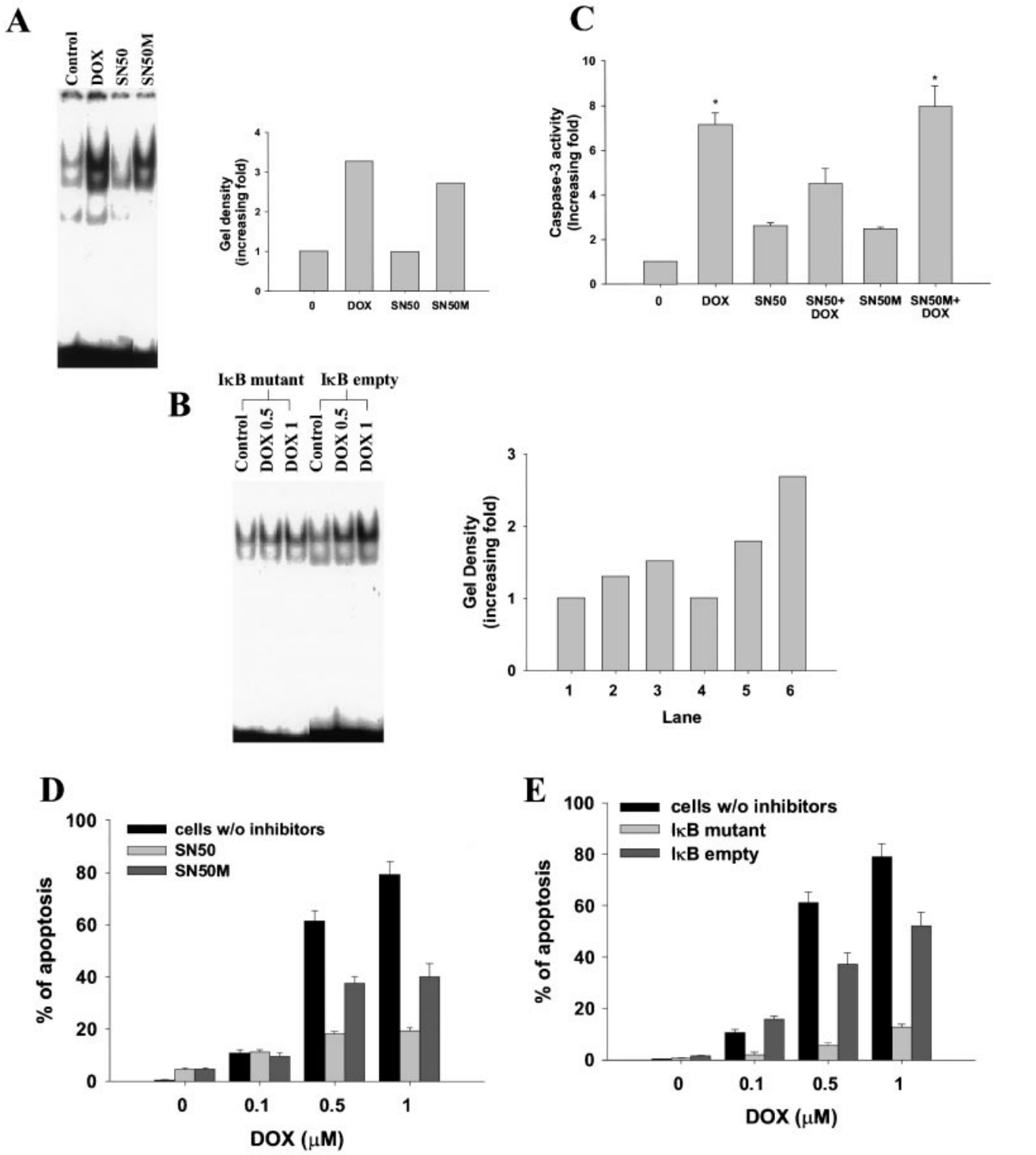

Figure 6 Blockade of NF-κB activation diminishes DOX-induced apoptosis

(**A**) The cells were pre-treated with 25 μg/ml NF-κB inhibitory peptide SN50 or control peptide SN50M for 30 min, followed by treatment with 0.5 μM DOX for 4 h. The nuclear extractions were collected for DNA-binding activity assay. (**B**) IκB mutant vector inhibited DOX-induced NF-κB activation. After being transfected with either IκB mutant vector or IκB empty vector, the cells were treated with 0.5 or 1 μM of DOX for 4 h. The nuclear extractions were collected for DNA-binding activity assay. (**C**) SN50 blocks DOX-induced caspase-3 activation. The cells were pre-treated with 25 μg/ml SN50 or SN50M for 30 min, followed by the treatment with 0.5 μM DOX for 16 h. The cell lysates were collected for caspase-3 activity assay. (**D**) SN50 blocks DOX-induced apoptosis. The cells were pre-treated with 25 μg/ml SN50 or SN50M for 30 min, followed by treatment with different concentrations of DOX for 16 h. TUNEL assay was performed for cell apoptosis. (**E**) IκB mutant vector blocks DOX-induced apoptosis. After being transfected with either IκB mutant vector or IκB empty vector, the cells were treated with different concentrations of DOX (0.1, 0.5 and 1 μM) for 16 h. Apoptosis was monitored by using the TUNEL assay.

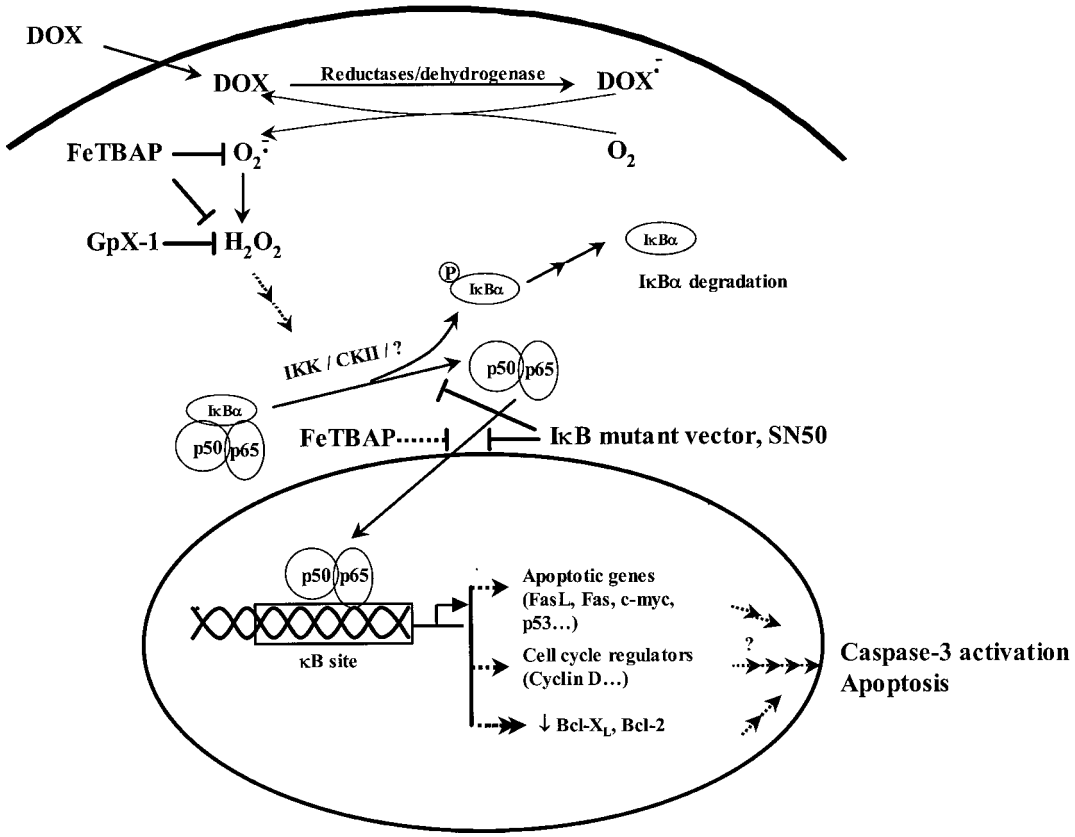

Scheme 1 A proposed scheme indicating DOX-induced activation and translocation of NF-κB into the nucleus, resulting in caspase activation and apoptosis

Overexpression of GPx-1 and supplementation with cell-permeant antioxidant enzyme-mimetic FeTBAP, SN50, a cell-permeant NF-κB inhibitory peptide or IκB mutant vector exert redox regulation at two levels: inhibition of H_2O_2-dependent activation of NF-κB and inhibition of NF-κB migration to the nucleus.

FeTBAP effectively scavenges the superoxide anion [39]. FeTBAP also decomposed H_2O_2 in a peroxidase-like mechanism (i.e. via formation of a perferryl-like species). The cytoprotective effects of FeTBAP and related metalloporphyrins have been attributed to their ability to detoxify superoxide, H_2O_2 and peroxynitrite [40,41]. From a mechanistic point, FeTBAP-mediated inhibition of NF-κB activity in cells is completely different from the inhibition of NF-κB by metal-ion chelators, e.g. pyrrolidine dithiocarbamate (PDTC)-type agents [42]. Transient transfection of GPx-1 expression plasmid into BAECs resulted in a dramatic decrease in NF-κB DNA-binding activity. GPx-1 overexpression abolished 2′,7′-dichlorofluorescin ('DCF') fluorescence (indicative of H_2O_2) and NF-κB activation, suggesting that H_2O_2 has a crucial role in DOX-induced NF-κB activation in endothelial cells and cardiomyocytes. Previously, using PDTC as an antioxidant and NF-κB inhibitor, it was concluded that ROS formation was not responsible for DOX-induced NF-κB activation in neuroblastoma cells [43]. This interpretation is not totally unambiguous, since PDTC is not a *bona fide* antioxidant [44]. Whereas PDTC can chelate redox-active metal ions (e.g. iron), its role as an ROS scavenger has been questioned [44].

Although H_2O_2 has been reported to cause NF-κB activation in several cell types in the presence of various oxidative stimuli, the exact mechanism by which NF-κB activity is regulated still remains unclear. Recently, it was shown that H_2O_2 could modulate the phosphorylation of IKKα subunit of IKK, the kinase responsible for IκB phosphorylation leading to further degradation [30]. Reports also indicate that 4-hydroxy-2-nonenal ('4-HNE'), a major lipid oxidation product, inhibits NF-κB activation by a covalent modification of IKK protein subunit [45]. In the present study, we did not observe any difference in the IKK activity in cells treated with or without DOX (results not shown). Whether other signal-transduction pathways, e.g. protein kinase CKII-mediated Tyr-42 phosphorylation and inhibition of protein phosphatases 1 and 2A, could have a role in DOX-induced NF-κB activation remains to be determined.

It is noteworthy that, in endothelial cells, NF-κB was not as readily activated by exogenously added H_2O_2 (results not shown). The activation of NF-κB could only be observed when cells were exposed to very high H_2O_2 levels (150 mM) for 4 h (results not shown). The differential induction of NF-κB by intra- and extracellular H_2O_2 suggests further that the oxidative stress induced by ROS depends on their site of generation and the levels of cellular antioxidants and antioxidant enzymes.

NF-κB has been reported to be involved in regulating DOX-induced apoptosis in various cancer cells and carcinomas, including breast-cancer cells, pancreatic carcinoma cells, leukaemia, lymphoma, renal carcinoma and hepatocellular carcinoma [16–18]. DOX-induced NF-κB activation in tumour cells is anti-apoptotic. Inhibition of NF-κB activation sensitizes cancer cells to DOX-induced apoptosis [16–18]. The present data provide evidence, for the first time, that NF-κB activation promotes DOX-induced apoptosis in vascular cells and myocytes. The pro-apoptotic character of NF-κB might be due to its direct activation of apoptotic genes, including Fas ligand, Fas, c-Myc and p53 [21,46,47]. Inhibition of NF-κB by SN50 was shown to inhibit

the activity of p53 and c-Myc, factors that are critical to mediating apoptotic signalling [47]. Another proposed mechanism is that NF-κB down-regulates the activities of some anti-apoptotic factors, e.g. Bcl-X_L [48]. In addition, the involvement of NF-κB in regulating the cell cycle can also be a mechanism for its pro-apoptotic effect [47].

The present study indicates that NF-κB activation is pro-apoptotic in endothelial cells and cardiomyocytes exposed to DOX. Published results using tumour cells demonstrate an anti-apoptotic role of NF-κB in DOX-induced apoptosis [16–18]. The dual role of NF-κB in regulating apoptosis may be used to enhance the therapeutic efficacy of DOX. NF-κB inhibitory chemicals could dramatically decrease the cardiac injury caused by DOX, but increase the sensitivity of cancer cells to DOX-induced apoptosis [30]. These cell-permeant SN50 peptides have been shown to systemically suppress the release of pro-inflammatory cytokines regulated by stress-responsive transcription factors including NF-κB [49]. The cell-permeable antioxidant FeTBAP, which protects endothelial cells and cardiomyocytes from DOX-induced apoptosis, reportedly has anti-inflammatory potential [40,41]. It is conceivable that the anti-apoptotic and anti-inflammatory effects of iron-based metalloporphyrins stem from their ability to inhibit NF-κB activation. It is unlikely that iron-based metalloporphyrins will affect NF-κB activation in tumour cells in response to DOX treatment, since the mechanism of DOX-mediated tumour cell killing is clearly very different. The present results suggest that iron-containing metalloporphyrins that inhibit stress-responsive transcription factors (e.g. NF-κB) [50] may be therapeutically used to mitigate DOX-induced apoptosis and cardiotoxicity.

This work was supported by the National Institutes of Health Grants 1PO1HL68769-01 and CA77822. We would like to thank Dr Yvonne Janssen-Heininger for many helpful discussions.

REFERENCES

1 Singal, P. K. and Iliskovic, N. (1998) Doxorubicin-induced cardiomyopathy. N. Engl. J. Med. **339**, 900–905
2 Buzdar, A. U., Marcus, C., Smith, T. L. and Blumenschein, G. R. (1985) Early and delayed clinical cardiotoxicity of doxorubicin. Cancer **55**, 2761–2765
3 Singal, P. K., Li, T., Kumar, D., Danelisen, I. and Iliskovic, N. (2000) Adriamycin-induced heart failure: mechanism and modulation. Mol. Cell Biochem. **207**, 77–86
4 Myers, C. E., McGuire, W. P., Liss, R. H., Ifrim, I., Grotzinger, K. and Young, R. C. (1977) Adriamycin: the role of lipid peroxidation in cardiac toxicity and tumor response. Science **197**, 165–167
5 Kalyanaraman, B., Perez-Reyes, E. and Mason, R. P. (1980) Spin-trapping and direct electron spin resonance investigations of the redox metabolism of quinone anticancer drugs. Biochim. Biophys. Acta **630**, 119–130
6 Davies, K. J. and Doroshow, J. H. (1986) Redox cycling of anthracyclines by cardiac mitochondria. I. Anthracycline radical formation by NADH dehydrogenase. J. Biol. Chem. **261**, 3060–3067
7 Kotamraju, S., Konorev, E. A., Joseph, J. and Kalyanaraman, B. (2000) Doxorubicin-induced apoptosis in endothelial cells and cardiomyocytes is ameliorated by nitrone spin traps and ebselen. Role of reactive oxygen and nitrogen species. J. Biol. Chem. **275**, 33585–33592
8 Sawyer, D. B., Fukazawa, R., Arstall, M. A. and Kelly, R. A. (1999) Daunorubicin-induced apoptosis in rat cardiac myocytes is inhibited by dexrazoxane. Circ. Res. **84**, 257–265
9 Wang, L., Ma, W., Markovich, R., Chen, J. W. and Wang, P. H. (1998) Regulation of cardiomyocyte apoptotic signaling by insulin-like growth factor. I. Circ. Res. **83**, 516–522
10 Laurent, G. and Jaffrezou, J. P. (2001) Signaling pathways activated by daunorubicin. Blood **98**, 913–924
11 Nakamura, T., Ueda, Y., Juan, Y., Katsuda, S., Takahashi, H. and Koh, E. (2000) Fas-mediated apoptosis in adriamycin-induced cardiomyopathy in rats: *in vivo* study. Circulation **102**, 572–578
12 Baeuerle, P. A. and Henkel, T. (1994) Function and activation of NF-κB in the immune system. Annu. Rev. Immunol. **12**, 141–179
13 Chen, F., Castranova, V., Shi, X. and Demers, L. M. (1999) New insights into the role of nuclear factor-κB, a ubiquitous transcription factor in the initiation of diseases. Clin. Chem. **45**, 7–17
14 Boland, M. P., Foster, S. J. and O'Neill, L. A. J. (1997) Daunorubicin activates NFκB and induces κB-dependent gene expression in HL-60 promyelocytic and Jurkat T lymphoma cells. J. Biol. Chem. **272**, 12952–12960
15 Aoki, M., Nata, T., Morishita, R., Matsushita, H., Nakagami, H., Yamamoto, K., Yamazaki, K., Nakabayashi, M., Ogihara, T. and Kaneda, Y. (2001) Endothelial apoptosis induced by oxidative stress through activation of NF-κB: antiapoptotic effect of antioxidant agents on endothelial cells. Hypertension **38**, 48–55
16 Arlt, A., Vorndamm, J., Breitenbroich, M., Folsch, U. R., Kalthoff, H., Schmidt, W. E. and Schafer, H. (2001) Inhibition of NF-κB sensitizes human pancreatic carcinoma cells to apoptosis induced by etoposide (VP16) or doxorubicin. Oncogene **20**, 859–868
17 Somerville, L. and Cory, J. G. (2000) Enhanced roscovitine-induced apoptosis is mediated by a caspase-3-like activity in deoxyadenosine-resistant mouse leukemia L1210 cells. Anticancer Res. **20**, 3347–3355
18 Manna, S. K. and Aggarwal, B. B. (1999) Lipopolysaccharide inhibits TNF-induced apoptosis: role of nuclear factor-κB activation and reactive oxygen intermediates. J. Immunol. **162**, 1510–1518
19 Joyce, D., Bouzahzah, B., Fu, M., Albanese, C., D'Amico, M., Steer, J., Klein, J. U., Lee, R. J., Segall, J. E., Westwick, J. K. et al. (1999) Integration of Rac-dependent regulation of cyclin D1 transcription through a nuclear factor-κB-dependent pathway. J. Biol. Chem. **274**, 25245–25249
20 Heermeier, K., Leicht, W., Palmetshofer, A., Ullrich, M., Wanner, C. and Galle, J. (2001) Oxidized LDL suppresses NF-κB and overcomes protection from apoptosis in activated endothelial cells. J. Am. Soc. Nephrol. **12**, 456–463
21 Hsu, S. C., Gavrilin, M. A., Lee, H. H., Wu, C. C., Han, S. H. and Lai, M. Z. (1999) NF-κB-dependent Fas ligand expression. Eur. J. Immunol. **29**, 2948–2956
22 Day, B. J., Shawen, S., Liochev, S. I. and Crapo, J. D. (1995) A metalloporphyrin superoxide dismutase mimetic protects against paraquat-induced endothelial cell injury, *in vitro*. J. Pharmacol. Exp. Ther. **275**, 1227–1232
23 Konorev, E. A., Zhang, H., Joseph, J., Kennedy, M. C. and Kalyanaraman, B. (2000) Bicarbonate exacerbates oxidative injury induced by antitumor antibiotic doxorubicin in cardiomyocytes. Am. J. Physiol. Heart Circ. Physiol. **279**, H2424–H2430
24 Pieper, G. M., Olds, C., Hilton, G., Lindholm, P. F., Adams, M. B. and Roza, A. M. (2001) Antioxidant treatment inhibits activation of myocardial nuclear factor kappa B and inhibits nitrosylation of myocardial heme protein in cardiac transplant rejection. Antioxid. Redox Signaling **3**, 81–88
25 Ye, J., Ghosh, P., Cippitelli, M., Subleski, J., Hardy, K. J., Ortaldo, J. R. and Young, H. A. (1994) Characterization of a silencer regulatory element in the human interferon-γ promoter. J. Biol. Chem. **269**, 25728–25734
26 Gavrieli, Y., Sherman, Y. and Ben-Sasson, S. A. (1992) Identification of programmed cell death *in situ* via specific labeling of nuclear DNA fragmentation. J. Cell Biol. **119**, 493–501
27 Nicholson, D. W. and Thornberry, N. A. (1997) Caspases: killer proteases. Trends Biochem. Sci. **22**, 299–306
28 Kalish, H., Camp, J. E., Stepien, M., Latos-Grazynski, L. and Balch, A. L. (2001) Reactivity of mono-*meso*-substituted iron(II) octaethylporphyrin complexes with hydrogen peroxide in the absence of dioxygen. Evidence for nucleophilic attack on the heme. J. Am. Chem. Soc. **123**, 11719–11727
29 Crow, J. P. (1999) Manganese and iron porphyrins catalyze peroxynitrite decomposition and simultaneously increase nitration and oxidant yield: implications for their use as peroxynitrite scavengers *in vivo*. Arch. Biochem. Biophys. **371**, 41–52
30 Li, Q., Sanlioglu, S., Li, S., Ritchie, T., Oberley, L. and Engelhardt, J. F. (2001) GPx-1 gene delivery modulates NFκB activation following diverse environmental injuries through a specific subunit of the IKK complex. Antioxid. Redox Signaling **3**, 415–432
31 Kalivendi, S. V., Kotamraju, S., Zhao, H., Joseph, J. and Kalyanaraman, B. (2001) Doxorubicin-induced apoptosis is associated with increased transcription of endothelial nitric-oxide synthase: effect of antiapoptotic antioxidants and calcium. J. Biol. Chem. **276**, 47266–47276
32 Golstein, P. (1997) Controlling cell death. Science **275**, 1081–1082
33 Green, D. R. and Reed, J. C. (1998) Mitochondria and apoptosis. Science **281**, 1309–1312
34 Schmidt, K. N., Amstad, P., Cerutti, P. and Baeuerle, P. A. (1995) The roles of hydrogen peroxide and superoxide as messengers in the activation of transcription factor NF-κB. Chem. Biol. **2**, 13–22
35 Wang, S., Leonard, S. S., Castranova, V., Vallyathan, V. and Shi, X. (1999) The role of superoxide radical in TNF-α induced NF-κB activation. Ann. Clin. Lab. Sci. **29**, 192–199
36 Shi, X., Dong, Z., Huang, C., Ma, W., Liu, K., Ye, J., Chen, F., Leonard, S. S., Ding, M., Castranova, V. and Vallyathan, V. (1999) The role of hydroxyl radical as a messenger in the activation of nuclear transcription factor NF-κB. Mol. Cell. Biochem. **194**, 63–70

37 Aggarwal, B. B. (2000) Apoptosis and nuclear factor-κB: a tale of association and dissociation. Biochem. Pharmacol. **60**, 1033–1039
38 Schreck, R., Albermann, K. and Baeuerle, P. A. (1992) Nuclear factor κB: an oxidative stress-responsive transcription factor of eukaryotic cells. Free Radical Res. Commun. **17**, 221–237
39 Kalyanaraman, B., Joseph, J., Bennett, B. and Konorev, E. A. (2001) Inhibition of doxorubicin-induced cardiomyocyte apoptosis by metalloporphyrins: is it due to ROS scavenging or Hsp induction? Free Radical Biol. Med. **31**, S1, S19
40 Misko, T. P., Highkin, M. K., Veenhuizen, A. W., Manning, P. T., Stern, M. K., Currie, M. G. and Salvemini, D. (1998) Characterization of the cytoprotective action of peroxynitrite decomposition catalysts. J. Biol. Chem. **273**, 15646–15653
41 Salvemini, D., Wang, Z. Q., Stern, M. K., Currie, M. G. and Misko, T. P. (1998) Peroxynitrite decomposition catalysts: therapeutics for peroxynitrite-mediated pathology. Proc. Natl. Acad. Sci. U.S.A. **95**, 2659–2663
42 Nathens, A. B., Bitar, R., Davreux, C., Bujard, M., Marshall, J. C., Dackiw, A. P., Watson, R. W. and Rotstein, O. D. (1997) Pyrrolidine dithiocarbamate attenuates endotoxin-induced acute lung injury. Am. J. Respir. Cell Mol. Biol. **17**, 608–616
43 Bian, X., McAllister-Lucas, L. M., Shao, F., Schumacher, K. R., Feng, Z., Porter, A. G., Castle, V. P. and Opipari, Jr, A. W. (2001) NF-κB activation mediates doxorubicin-induced cell death in N-type neuroblastoma cells. J. Biol. Chem. **276**, 48921–48929
44 Moellering, D., McAndrew, J., Jo, H. and Darley-Usmar, V. M. (1999) Effects of pyrrolidine dithiocarbamate on endothelial cells: protection against oxidative stress. Free Radical Biol. Med. **26**, 1138–1145
45 Ji, C., Kozak, K. R. and Marnett, L. J. (2001) IκB kinase, a molecular target for inhibition by 4-hydroxy-2-nonenal. J. Biol. Chem. **276**, 18223–18228
46 Chan, H., Bartos, D. P. and Owen-Schaub, L. B. (1999) Activation-dependent transcriptional regulation of the human Fas promoter requires NF-κB p50/p65 recruitment. Mol. Cell. Biol. **19**, 2098–2108
47 Qin, Z. H., Chen, R. W., Wang, Y., Nakai, M., Chuang, D. M. and Chase, T. N. (1999) Nuclear factor κB nuclear translocation upregulates c-Myc and p53 expression during NMDA receptor-mediated apoptosis in rat striatum. J. Neurosci. **19**, 4023–4033
48 Hettmann, T., DiDonato, J., Karin, M. and Leiden, J. M. (1999) An essential role for nuclear factor κB in promoting double positive thymocyte apoptosis. J. Exp. Med. **189**, 145–158
49 Liu, R. Y., Fan, C., Olashaw, N. E., Wang, X. and Zuckerman, K. S. (1999) Tumor necrosis factor-α-induced proliferation of human Mo7e leukemic cells occurs via activation of nuclear factor κB transcription factor. J. Biol. Chem. **274**, 13877–13885
50 Rong, Y., Doctrow, S. R., Tocco, G. and Baudry, M. (1999) EUK-134, a synthetic superoxide dismutase and catalase mimetic, prevents oxidative stress and attenuates kainate-induced neuropathology. Proc. Natl. Acad. Sci. U.S.A. **96**, 9897–9902

Received 10 May 2002/15 July 2002; accepted 25 July 2002
Published as BJ Immediate Publication 25 July 2002, DOI 10.1042/BJ20020752